Tracking Conformational States in Allosteric Transitions of Phosphorylase†

Michelle F. Browner,* Eric B. Fauman, and Robert J. Fletterick*

Department of Biochemistry and Biophysics, University of California, San Francisco, California 94141-0448

Received February 4, 1992; Revised Manuscript Received August 19, 1992

ABSTRACT: An intrinsic molecular property of a protein domain can be determined by calculating its principal axes from the inertia tensor matrix. The mass-weighted principal axes can be used to calculate an ellipsoid representing the shape of the protein domain, providing an easy means of visualizing domain movements. Most importantly, the mass-weighted principal axes provide an intuitive means of characterizing domain relationships within a protein, as well as the disposition of domains in different protein conformers. Thus, this method provides a simple, quantitative description of differences of domain positions within various protein structures. We show the utility of this method by characterizing the quaternary and tertiary differences as observed in eight structures of phosphorylated or dephosphorylated glycogen phosphorylase with different effectors bound. This analysis revealed domain movements which were characteristic of the activated phosphorylase structures. The monomers of the phosphorylase dimer were found to move apart by a 2.5-Å translation and to rotate apart, in three orthogonal directions, by a minimum of 3.2°. Analysis of the three domains within the phosphorylase monomer showed that both simple and complex domain movements occur and that multiple domain configurations are energetically stable. We suggest that the C-terminal domain of phosphorylase moves along a simple path in the transition from an inactive to active conformation. The direction of translation and rotation is consistent, but the magnitude is variable. In contrast, this analysis showed that the activation domain did not behave as a rigid body, and therefore, the motion of this domain is not as easily characterized.

The Monod–Wyman–Changeaux (MWC) theory of allostery defined two conformational states of a protein, one inactive (T) and the other active (R) (Monod et al., 1965). The transition between the two conformations is achieved by ligand binding, and the resulting conformer of the protein–ligand complex is the one with the lowest free energy. Allosteric effectors can either activate or inhibit enzymatic activity by altering the equilibrium between these two states. A kinetic model derived according to MWC theory for rabbit muscle glycogen phosphorylase fits experimental observations (Madsen, 1986). The ratio of [T] to [R] is shifted toward the activated state when AMP is bound, and the associated conformational change increases the affinity of the enzyme for its substrates. When activated by the covalent phosphorylation of serine 14, phosphorylase is no longer subject to allosteric control by AMP. The phosphorylated enzyme displays allosteric behavior only when an inhibitor, such as glucose, is present to stabilize the T state. The equilibrium constant for the ratio of [T] to [R] of the unliganded, phosphorylated enzyme significantly favors the activated conformer, as a result of structural changes associated with phosphoserine interactions (Sprang et al., 1988).

X-ray crystallographic analysis has been used to determine atomic coordinates for more then a dozen chemically or conformationally distinct states of muscle phosphorylase. Describing the spatial relationships of domains within these different structures has proven to be a difficult task. A comparison of the phosphorylated and dephosphorylated proteins (Sprang et al., 1988) provided a set of important atomic differences to consider in evaluating other phosphorylase structures. What has been lacking, however, is a simple, quantitative means of measuring quaternary and tertiary changes associated with the T to R transition. Indeed, the most popular means of describing protein domain movements involves superpositioning algorithms. When applied to phosphorylase, this method has led to strikingly different interpretations [for example, Barford and Johnson (1992) and Goldsmith et al. (1989)].

In this report we describe a method for measuring tertiary and quaternary structural changes of domains within a protein. The algorithm provides an easy test of the domain definition as a rigid body and allows distinct states in a protein crystal to be defined and compared between different structures. The method is general and permits the accurate description of small conformational changes due to amino acid substitutions or the binding of ligands. We apply the method to eight atomic coordinate sets of glycogen phosphorylase to define a complex spectrum of domain shifts involved in the allosteric transition between the T and R states.

EXPERIMENTAL PROCEDURES

Principal Axes Determination. A rigid body is defined in mechanics as a collection of particles whose relative positions are fixed by constraints. The principal axes of a rigid body are those about which it can be rotated without external torque. A set of three mutually orthogonal principal axes can be determined by constructing and diagonalizing the inertia tensor of the object. The tensor is readily constructed from classical mechanics (Goldstein, 1950); the diagonal elements of the inertia tensor, **I**, are

$$\mathbf{I}_{xx} = \sum_{i=1}^{n} m_i(\mathbf{r}_i^2 - x_i^2) \qquad \mathbf{I}_{yy} = \sum_{i=1}^{n} m_i(\mathbf{r}_i^2 - y_i^2)$$

$$\mathbf{I}_{zz} = \sum_{i=1}^{n} m_i(\mathbf{r}_i^2 - z_i^2)$$

† This work was supported by Grant DK26081 from the National Institutes of Health (to R.J.F). E.B.F. is a Howard Hughes Medical Institute Predoctoral Fellow.

* Authors to whom correspondence should be addressed.

0006-2960/92/0431-11297$03.00/0

and off-diagonal elements are given by

$$\mathbf{I}_{xy} = -\sum_{i=1}^{n} m_i x_i y_i \text{ etc.}$$

where n is the number of mass elements in the object, m_i is the mass of the ith element, $\mathbf{r}_i$ is the position vector from the center of mass to the ith point, and x_i, y_i, and z_i are the x, y, and z components of the vector $\mathbf{r}_i$.

The principal moments and the principal axes are the eigenvalues and eigenvectors, which derive from diagonalization of the inertia tensor. The eigenvectors $\mathbf{v}_1$, $\mathbf{v}_2$, and $\mathbf{v}_3$ satisfy the equations

$$\mathbf{I}\mathbf{v}_k = \lambda_k \mathbf{v}_k \quad \text{for } k = 1, 2, 3$$

where λ_k are the principal moments.

We have used the three principal axes to mathematically describe protein domains, summing over selected atomic positions. In order to generate axes which accurately describe the shape of a protein domain, the distribution of mass along each axis was included to weight the vectors using the equation

$$V_k = \left(\sum_{i=1}^{n} m_i (r_i \cdot \mathbf{v}_k)^2 / \sum_{i=1}^{n} m_i\right)^{1/2} \quad \text{for } k = 1, 2, 3$$

The shape-weighted principal axes **L**, **M**, and **S** were defined by weighting the unit eigenvectors, $\mathbf{v}_k$, by the mass distribution, V_k. **L** was set to $V_k\mathbf{v}_k$, for the largest value of V_k. Likewise, **M** was assigned to the middle value and **S** to the smallest value of V_k. Thus, the lengths of the three principal axes are weighted by the mass distribution projected along the corresponding axis.

This principal axes algorithm (a component of GEM; E. Fauman, in preparation) returns the center of mass of the polypeptide domain, as well as the eigenvectors ($\mathbf{v}_k$) and the shape-weighted lengths (V_k). The coordinates for the shape-weighted principal axes were viewed using INSIGHTII (Biosym Technologies). A useful construction of the domain defined by three principal axes was created by generating ellipsoids (Figure 1C) defined by the equation

$$1 = x^2\frac{\mathbf{L}}{|\mathbf{L}|} + y^2\frac{\mathbf{M}}{|\mathbf{M}|} + z^2\frac{\mathbf{S}}{|\mathbf{S}|}$$

A similar approach has been used to represent the shape of a protein as an ellipsoid (Taylor et al., 1983), where the ellipsoid was arbitrarily scaled to encompass a specified percentage of the protein atoms. In the present study, the ellipsoid which represents the protein domain as described by the mass-weighted axes was scaled by $\sqrt{5}$, the scale factor required to return the full-size ellipsoid defined by a principal axes calculation.

Phosphorylase Structures. Atomic coordinates for eight different rabbit muscle phosphorylase crystal structures, determined in our laboratory and by L. N. Johnson and coworkers, were used in the analysis (Table I). The structures are of the phosphorylated (serine-14 phosphate, PA, PAMP, GP) or dephosphorylated (PB, P48T, P48G, PB4, PLPP) forms of phosphorylase with different ligands bound. Two of the structures (P48T and P48G) are of mutant phosphorylase proteins in which proline 48 was replaced with either threonine or glycine. Six of the eight structures were determined from a tetragonal crystal form with the same space group and unit cell constants within 1.5% of each other. This crystal form has a single phosphorylase monomer in the asymmetric unit. The other two structures were determined from two different, nonisomorphous crystals each with four monomers in the asymmetric unit.

Domain Definitions. Historically, the phosphorylase monomer has been divided into two loosely defined domains. The first 482 amino acid residues are referred to as the N-terminal domain and the second half of the polypeptide chain (amino acids 483–842) the C-terminal domain [see, for example, Browner and Fletterick (1992)]. Recently, Sprang et al. (1991) subdivided the N-terminal domain, defining amino acids 1–120 as the activation domain. These domains are contiguous in sequence. The eight structures were visually compared, and the three domain definitions were refined for this analysis. Segments of the protein chain absent from any one of the refined structures were eliminated. For example, no electron density was observed for amino acids 264–289 in the PLPP map, and these residues were, therefore, excluded from the N-terminal domain. Loops or short-chain segments that were mobile due to local positional differences in the various structures were also not included in the definitions. Finally, residues with high crystallographic temperature factors (50.0 Å^2) were deleted. The atoms in each domain definition are found in all eight structures.

Using these criteria, the activation domain was defined by 83 amino acid residues: 23–25, 28–62, 66–75, 77–78, 83–102, and 107–120. The N-terminal domain consists of 178 residues: 190–195, 197–204, 215–221, 223–228, 241–247, 290–314, 328–337, 340–359, 366–377, 385–405, 409–414, 416–417, 426–427, 429–432, 435–455, 457–460, 462–470, and 473–480. The C-terminal domain contains 321 residues: 485–496, 498–500, 502–508, 510–519, 521–548, 556–567, 570–594, 596–649, 652–671, 678–683, 685–694, 696–745, and 747–813. For this analysis, the phosphorylase monomer consists of the sum total of the amino acid residues in the activation, N-terminal, and C-terminal domains, 582 amino acids.

Principal Axes Comparisons. As implemented, the principal axes determination describes the orientation of one domain or monomer relative to another. The disposition of one set of principal axes relative to another is described by the difference in the center of mass and by the angles between the sets of principal axes, **L**, **M**, and **S**. For example, the angle between the two **L** vectors is

$$\theta_L = \arccos \frac{\mathbf{L}_1\mathbf{L}_2}{|\mathbf{L}_1||\mathbf{L}_2|}$$

The center of mass and the three principal axes for the activation, N-terminal, and C-terminal domains defined for each phosphorylase structure were determined using only α-carbon coordinates from the independently refined structures (Table I). Each α-carbon position was equally weighted in the mass determinations. The relative positions of each pair of identical domains in the phosphorylase dimer, activation domains (AA′), N-terminal domains (NN′), and C-terminal domains (CC′), were compared. The prime notation (′) indicates the domain in the 2-fold symmetry-related monomer. The relative positions of each pair of domains within the phosphorylase monomer, activation versus N-terminal domain (A/N), activation versus C-terminal domain (A/C), and N-terminal versus C-terminal domain (N/C), were analyzed. The monomers of each phosphorylase dimer were also compared.

The results are presented by comparing seven phosphorylase structures (P48T, P48G, PA, PAMP, GP, PB4, PLPP) to PB, the dephosphorylated, unliganded muscle phosphorylase. For example, the center of mass separation and the three angles which describe the relationship of the activation domain to the N-terminal domain in P48T were subtracted from the

Table I: Characteristics of Phosphorylase Crystal Structures and Refinement

name	ligands[a]	crystal buffer[b]	space group	unit cell (Å)	AU	refinement	res (Å)	R-factor	ref
PB		10 mM $Mg(OAc)_2$, 1 mM IMP	$P4_32_12$	$a = b = 128.5$, $c = 116.3$	monomer	PROLSQ	1.9	0.19	Acharya et al., 1991
P48T		10 mM $Mg(OAc)_2$, 1 mM AMP	$P4_32_12$	$a = b = 128.5$, $c = 116.3$	monomer	PROLSQ	2.7	0.20	Browner et al., 1992
P48G		10 mM $Mg(OAc)_2$, 1 mM AMP	$P4_32_12$	$a = b = 128.5$, $c = 116.3$	monomer	PROLSQ	2.8	0.19	Browner et al., 1992
PA	Ser 14-PO_4, glucose	10 mM $Mg(OAc)_2$, 50 mM glucose	$P4_32_12$	$a = b = 128.4$, $c = 116.4$	monomer	PROLSQ	2.1	0.15	[c]
PAMP	Ser14-PO_4, glucose, AMP (soak)	10 mM $Mg(OAc)_2$, 50 mM glucose	$P4_32_12$	$a = b = 128.3$, $c = 117.0$	monomer	PROLSQ	2.5	0.12	Sprang et al., 1987
GP	Ser14-PO_4, maltopentaose, Glc-1-P (soak)	10 mM $Mg(OAc)_2$, 50 mM glucose	$P4_32_12$	$a = b = 128.5$, $c = 118.1$	monomer	PROLSQ	2.8	0.19	Goldsmith et al., 1989
PB4	sulfate	1.0 M $(NH_4)_2SO_4$, 10 mM glycerophosphate	$P2_1$	$a = 119.0$, $b = 190.0$, $c = 88.2$, $\beta = 109.4°$	tetramer	XPLOR	2.9	0.18	Barford & Johnson, 1989
PLPP	AMP, pyrophosphate	4% PEG 2.5 mM $Mg(OAc)_2$, 0.5 mM AMP	$P2_12_12$	$a = 169.8$, $b = 209.9$, $c = 123.4$	tetramer	XPLOR	3.0	0.18	Sprang, 1991

[a] Ligands as determined by their presence in the electron density map. [b] Crystal buffers were all about pH 7.0, and other additives such as EDTA and DTT were present. [c] S. Sprang, E. Goldsmith, and R. Fletterick, unpublished results.

same quantities which describe the disposition of these domains in PB. It is in this comparison that the movements of the domains become signed, and the sign represents the direction of movement relative to PB, only. The center of mass values report the separation (in angstroms) between two domains. The angles derived from comparing the same domains within the dimer were halved (AA′, NN′, CC′); thus the values reported correspond to the angular movement of a single domain.

RESULTS

The enzymatic activity of glycogen phosphorylase is differentially affected by activators such as AMP or covalent phosphorylation and by the presence of inhibitors (glucose) or substrates (maltoheptaose). Table I lists the phosphorylase structures used in this analysis in a nonarbitrary order based on presumed activation state. The rationale for the list of the phosphorylase structures, from the most T-state structure to the most R-like structure, is as follows: PB is the structure of the dephosphorylated, unliganded enzyme and is considered to be the most inactive structure (Acharya et al., 1991). P48T and P48G contain single amino acid substitutions at position 48 and were crystallized in the same condition as PB. Both P48T and P48G bind AMP noncooperatively, which in the case of P48G leads to an enzyme that is hyperactivated (Browner et al., 1992). PA is the structure of the enzyme with serine-14 phosphate and the inhibitor, glucose, bound (S. Sprang, E. Goldsmith, and R. Fletterick, unpublished results). This enzyme would be inactive because the active site inhibitor is present, but the structural conformation has been moved toward the R state by covalent activation. PAMP was obtained from PA crystals soaked in AMP with glucose present (Sprang et al., 1987). Enzymatically this protein would also be inactive, but in the absence of glucose, PAMP would be more active than PA (Madsen, 1986). GP was obtained from another soaking experiment where glucose was soaked out of the PA crystal and substrates, orthophosphate and maltopentaose, were soaked in, and the maltopentaose was found at the glycogen storage site (Goldsmith et al., 1989). This enzyme has full enzymatic activity in solution (Kasvinsky et al., 1978), although crystal-packing forces have likely restrained the conformational changes (Kasvinsky & Madsen, 1976).

Phosphorylase is activated by sulfate, which mimics phosphate. PB4 is the structure of the dephosphorylated enzyme crystallized as a tetramer in the presence of sulfate; the sulfate ion was found in the three known phosphate binding sites (Barford & Johnson, 1989). Sulfate activates phosphorylase by binding at the AMP site or the binding site for serine-14 phosphate but would inhibit enzymatic activity when bound at the active site. PLPP, the last structure on the list, is also from a tetrameric crystal form of the dephosphorylated enzyme grown in the presence of poly(ethylene glycol). In this structure, AMP is bound at the activation site, and the coenzyme pyridoxal phosphate is replaced by a transition-state analog, pyridoxal pyrophosphate (Sprang et al., 1991).

Phosphorylase Domains. Figure 1A shows the α-carbon trace of a phosphorylase dimer and the principal axes which define the disposition of the activation, N-terminal, and C-terminal domains. The N- and C-terminal domains were shown to move as rigid bodies, whereas the activation domain was observed to change size slightly. The deformation of each domain was quantified by the change in length of the shape-weighted axes. The lengths of the C-terminal domain axes for all the structures were within 0.04 Å of the lengths for PB. The deformation of the N-terminal domains was similarly small for the group of structures, with the largest change being 0.11 Å in the GP structure. This is the only structure in this analysis with oligosaccharide bound at the glycogen storage site. Only the long axis of the activation domain showed larger variations. This axis shortened by an average of 0.13 Å when the protein was phosphorylated (PA, PAMP, GP) and by 0.21 and 0.18 Å in the two tetrameric structures (PB4 and PLPP). Sprang et al. noted that the length of the helix containing amino acids 48–76, which is nearly parallel with the L axes of the activation domain, shortens on activation by phosphorylation (Sprang et al., 1988).

Quaternary Structural Changes. The quaternary structural changes relative to PB, described by the center of mass separation and moment of inertia vectors, for the monomers of each phosphorylase dimer in Table I, are presented in Figure 2. A positive value for the change in center of mass separation implies that the monomers have moved closer together relative to their position in PB, whereas a negative value indicates increasing separation. In the potentially most activated structures (PB4 and PLPP), the separation of the center of mass of the monomers has increased by 2.5 Å, relative to the separation in PB. The changes in the three angles that define the relative orientation of the principal axes of the monomers (Figure 2B) were similarly greatest for these structures. The largest change corresponds to a rotation of −3.3°, −4.1°, and −3.7° for the L, M, and S axes of PLPP. The negative sign

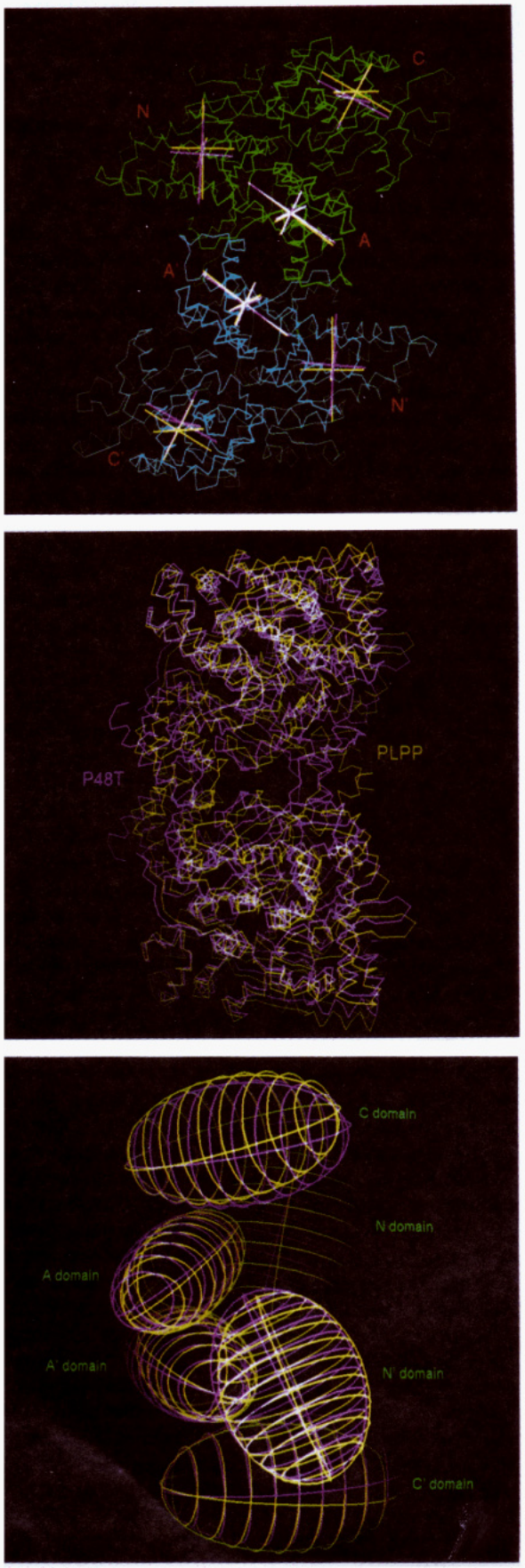

FIGURE 1: Quaternary structural change in phosphorylase. (A, top) The α-carbon ribbon trace of the inactive phosphorylase dimer as determined for P48T (Browner et al., 1992). The principal axes for the activation, N-terminal, and C-terminal domains for both P48T (pink) and PLPP (yellow) are shown, and the three domains of the dimer are labeled (A, A′, activation domain; N, N′, N-terminal domain, C, C′, C-terminal domain). (B, middle) The α-carbon trace of P48T (pink) and PLPP (yellow) (Sprang et al., 1991) superimposed using the same atoms as in the principal axes analysis. The phosphorylase dimer is turned 90° relative to the view in part A. (C, bottom) The ellipsoids for each domain of the phosphorylase dimer, for both P48T (pink) and PLPP (yellow), are shown in the same orientation as in part B.

of all the angular movements, in PB4 and PLPP relative to PB, implies that the phosphorylase monomers rotate away from each other. The three phosphorylated molecules (PA, PAMP, GP) show smaller differences in the **M** and **S** angles, although in the same negative direction. The **L**-axes angles also change, but in the opposite (positive) direction. The movement of the monomers in other structures is virtually nonexistent.

Tertiary Structural Changes. Analysis of the individual domain movements of phosphorylase consisted of six comparisons (Figures 3–5). In the dimer, the disposition of the analogous domains (AA′, NN′, and CC′; Figures 3A and 4) was compared, and within the monomer, each domain was compared to each of the other domains (A/N, A/C, and N/C; Figures 3B and 5).

(*A*) *Translational Differences.* The center of mass separation of like domains in the phosphorylase dimer is given as a difference in separation relative to PB (Figure 3A). The separation of the activation domains (AA′) shows the largest decrease, +0.9 Å, in the phosphorylated structures (PA, PAMP, and GP), indicating the activation domains move toward each other. The same direction of movement was seen for the dephosphorylated, active structures (PB4 and PLPP), but the movement was less (+0.6 Å). The separation of N-terminal domains in the structure with substrate bound (GP) decreases relative to PB (+0.5 Å), whereas in the dephosphorylated, tetrameric structures (PB4 and PLPP), the N-terminal domains move apart by −1.0 Å. The C-terminal domains also move apart in the case of PAMP, GP, PB4, and PLPP. In the enzymatically most active structures these domains move apart by 3.6 Å.

The movements of the center of mass for domains within a phosphorylase monomer are shown in Figure 3B. The degree of movement was the largest for A/C and N/C. The N- and C-terminal domains move apart by 1.0 Å in PLPP and 0.7 Å in PB4. The separation of the activation and C-terminal domains, however, increases more in the phosphorylated structures (PA, PAMP, and GP) than in PLPP. The relative movement of the activation and N-terminal domains (A/N) was much less in all structures. The largest change in these domains was 0.25 Å in PLPP, in the positive direction, indicating that the activation and N-terminal domains move slightly toward each other.

(*B*) *Rotational Differences.* The disposition of the domains within the phosphorylase dimer can also be described by the change in the angles of the principal axes of each domain (Figure 4). The sign of angular movement of each principal axis represents the direction of the movement with reference to the ground-state structure (PB). For example, the rotations of the principal axes of the activation domains in PA and PAMP are all in the positive direction relative to PB (Figure 4, AA′). The positive direction of all the angular differences implies that the domains have rotated toward each other, relative to their position in PB. When the signs of the relative motion of the three axes are not the same, the description of the motion is less intuitive. The movements of the **L** axes for the activation domains of PB4 and PLPP were also in the same direction, but of greater magnitude, whereas the **M** and

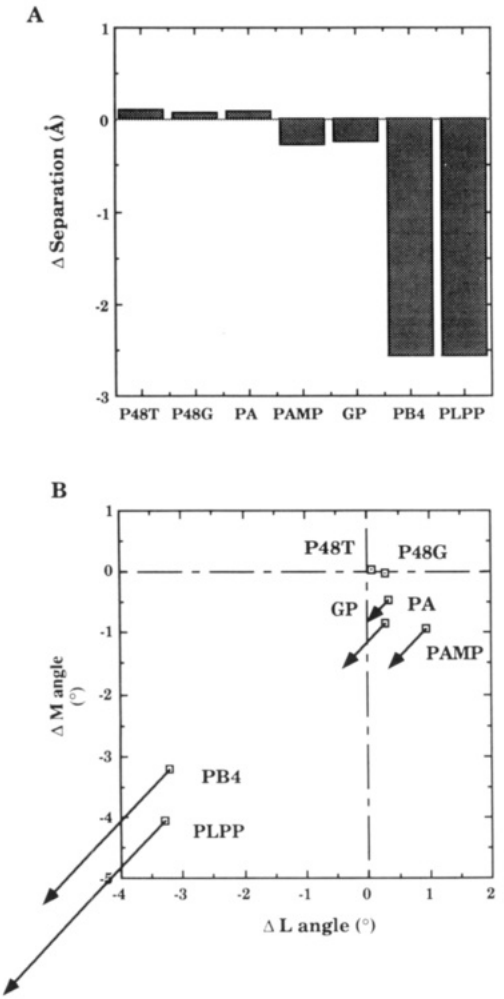

FIGURE 2: Movement of the center of mass and rotation of the principal axes in the quaternary structural change. (A) The distance between the centers of mass of the PB monomers is compared to the separation of the monomers in the seven other structures. The *y* axis of the bar graph shows the relative center of mass movement in angstroms. (B) The changes in rotational orientation of the subunits due to quaternary movements are characterized by changes in interaxes angles (**L** vs **L**, **M** vs **M**, **S** vs **S**) between monomers. A two-dimensional graph represents the three angular differences. The difference between the angle determined by the **L** axes of PB monomers and that of the other structures is indicated along the abscissa, and the ordinate shows the **M**-axes angle comparison. The **S**-axes angle change is shown by the magnitude and direction (positive or negative) of the arrow originating from the point positioned according to the **L** and **M** angle changes. The scales for **L**, **M**, and **S** are equivalent. The arrow is arbitrarily positioned 45° relative to the abscissa and ordinate axes. A positive change in **S** is noted by an arrow pointing to the upper right corner and a negative change by an arrow pointing to the lower left corner.

S axes rotated in the negative direction. For the N-terminal domains of the dimer (Figure 4, NN′) the rotational movements of the **L** and **M** axes were all in the positive direction. In the most active enzymes (PB4 and PLPP) the N-terminal domains rotate toward each other by 5° from the position of the **L** and **M** axes in PB. The most significant movement of the C-terminal domains (Figure 4, CC′) was in PLPP where the domains rotate away from each other: –5.3° with respect to **L**, –2.7° with respect to **M**, and –6.6° with respect to **S**.

Figure 5 shows the results from a similar analysis of domain rotations, where domains within a monomer of phosphorylase were examined. The angular movements of the heterologous domains appear to be more complicated in that none are characterized by angles that all move in the positive or negative direction.

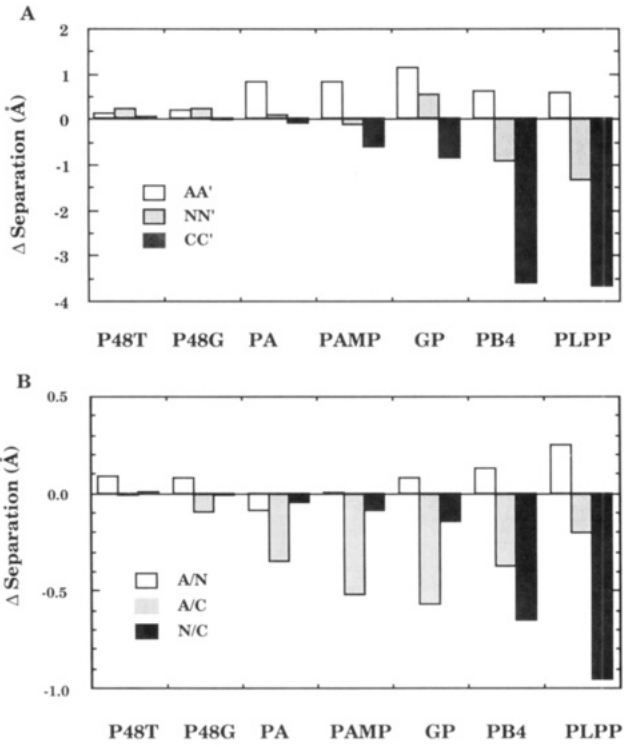

FIGURE 3: Domain center of mass movements. The change in the separation of the domains in the dimer (A) and the monomer (B) is shown. The three domains described are activation (A), N-terminal (N), and C-terminal (C). The ordinate shows the relative movement in angstroms.

Estimation of the Error. The reliability of measuring conformational changes by the principal axes method was determined from a comparison of independently refined structures of phosphorylase and rat anionic trypsin, a protein not expected to have conformational differences. The differences in the center of mass positions of domains in mutant phosphorylase (P48T and P48G) and the trypsin structures were 0.01 Å. A principal axes analysis of N- and C-terminal domains of trypsin indicated that the error in determining the rotational positions of the axes was, on average, less than 0.13°.

DISCUSSION

Defining Conformational Changes in Proteins. Large-scale conformational changes in proteins can be determined experimentally by several physical methods including spectroscopy, nuclear magnetic resonance, small-angle scattering, and X-ray crystallography. When crystals exist for various conformers of a large protein, crystallography provides the highest resolution data and, therefore, the most accurate method for defining these changes. From such crystallographic data it is possible to describe at an atomic level the positional changes observed in different protein conformations (Sprang et al., 1988). When the atomic differences involve the movement of 842 amino acids, as in the case of phosphorylase, the description, unfortunately, becomes confusing and very difficult to quantitate. In such cases, the conformational changes have historically been characterized by superimposing subsets of atoms from the different protein structures and computing the rotation and translation matrices that relate the protein domains (Hendrickson, 1979; Matthews & Rossman, 1985; Rossman & Argos, 1975). The atomic members of the subsets are adjusted to find the most rigid core. The data returned from a superposition program include angle representations of the magnitude of the rotation and the

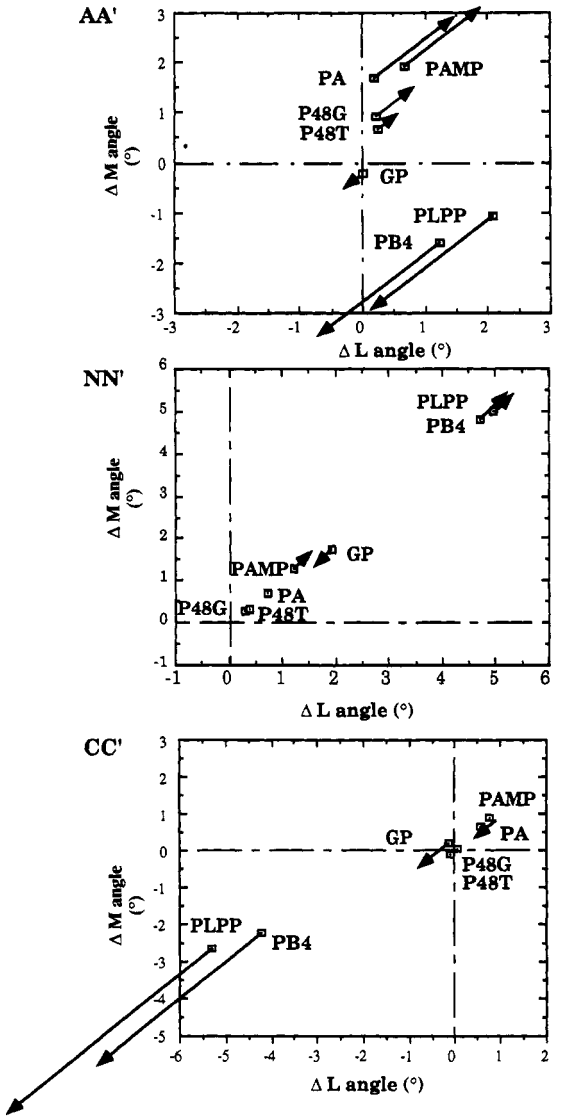

FIGURE 4: Angular movements of the domains in the dimer. The two-dimensional graphs represent the change in axes angles as described in Figure 2B. The comparison is between the activation domains (AA'), the N-terminal domains (NN'), and the C-terminal domains (CC') for each structure relative to PB.

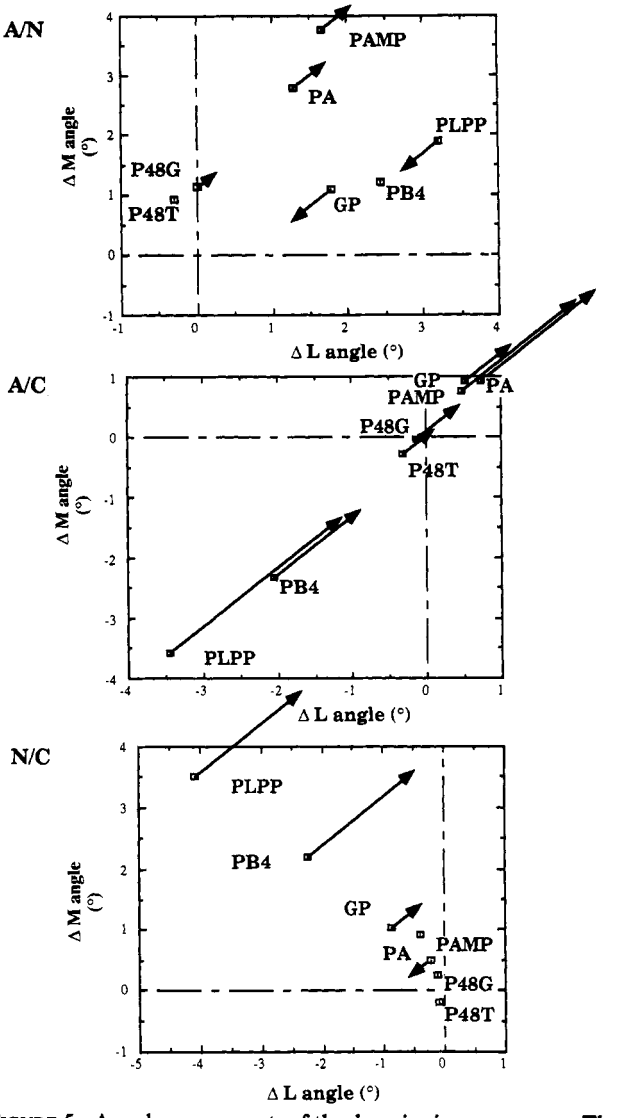

FIGURE 5: Angular movements of the domains in a monomer. The two-dimensional graphs represent the change in axes angles as described in Figure 2B. A/N shows the comparison between the activation and N-terminal domains, A/C between the activation and C-terminal domains, and N/C between the N-terminal and C-terminal domains.

translation vectors. Diagonalization of the transformation matrix provides the direction cosines of the rotation axis and its position, as well as the magnitude of the rotation (Muirhead et al., 1967). This kind of procedure accurately reports the rotational and translational matrix which superimposes an identical set of atoms from two structures. A small, but significant, rotation (1°) of the C-terminal domain was found by this method in the comparison of the dephosphorylated (PB) and phosphorylated (PA) crystal structures (Sprang et al., 1988). The superposition method is also commonly used to define an axis about which a hingelike motion takes place (Bystroff & Kraut, 1991).

Both the superpositioning algorithm and the principal axes method describe the relationship of protein domains using distance and angular values. There are, however, major differences between these methods. The transformation matrix and vector derived from a superposition algorithm provide a complete description of the screw axis relating two structures. The principal axes method does not calculate a transformation matrix but rather provides a measure of change between domain conformations. The relative disposition of one domain to another is described by the center of mass shift and three angular values which describe the rotational motion of the principal axes. These four values are then used to quantitate the domain motions in different conformational states relative to a ground-state structure. The descriptions of protein motion given by the superposition or principal axes method are both very accurate, but they are different. The superposition method has been used to describe the movements of the N-terminal (corresponds to the activation domain) and C-terminal subdomains of phosphorylase upon tetrameric association (Barford & Johnson, 1992). This description involves defining the screw axes about which each domain rotation occurs. Often, a screw axis will drift in position and orientation when several different structures are compared, making an assessment of the conformational dynamics difficult (Bystroff & Kraut, 1991). The method described here can be used to quantitate domain movements in many different structures. Furthermore, by assignment of a reference structure, the progression of domain movements can be examined.

The mass weighting of the principal axes is unique to our method (Figure 1A). The assumption of a fixed tertiary structure within a domain can be evaluated by the equality of the lengths of the mass-weighted principal axes component

vectors. Although the principal axes method does not provide an automated means of accurately determining protein domains, it does test the validity of user-defined domains as rigid bodies. The mass-weighted principal axes also allow for an accurate graphic abstraction of the described protein domain as an ellipsoid (Figure 1C). This graphical representation is analogous to the moment ellipsoid defined previously (Taylor et al., 1983), with one difference. In the earlier study, the moment of inertia ellipsoid was arbitrarily scaled to encompass a defined percentage of the protein atoms. The ellipsoid defined by the mass-weighted principal axes is scaled by a nonarbitrary factor determined from geometric constraints.

Conformational Changes in Phosphorylase. The principal axes method provides a simple means of looking for continuity of change along specific pathways in three-dimensional space. Using eight phosphorylase crystal structures, domain movements involved in the T to R transition were revealed. The three domains that were analyzed are not the only domains into which the phosphorylase monomer can be divided. A glycogen binding domain has also been described (Goldsmith et al., 1982, 1989). The activation, N-terminal, and C-terminal domains, however, were chosen to provide a simple view of the conformational changes which occur during the T to R transition. Importantly, the principal axes analysis showed that, for these three, the domain definitions were reasonable in that the change in the axes lengths was small. The absence of tertiary deformation implies that the N- and C-terminal domains move as rigid units, as expected for well-defined domains. The activation domain, however, undergoes larger alterations in its tertiary structure.

In this analysis we considered six structures determined from phosphorylase crystals which display similar packing contacts with slightly different lattice constants. The two structures, PB4 and PLPP, which have the largest conformational changes belong to totally different crystal systems (Table I). We expect, however, that the conformational changes associated with the bound effectors in these two structures would dominate any effect due to crystal-packing forces. This hypothesis is supported by the observation that structures from the different space groups exhibit a progression of domain movements (for example, see Figure 5).

All conformational changes are described relative to the T state as found in the PB structure (Acharya et al., 1991). The principal axes analysis confirmed that the largest quaternary structural changes reported thus far are observed in the PLPP structure which is activated by AMP (Sprang et al., 1991). Along all three axes, a large (3–4°) rotation moves the two monomers apart, and the separation of the monomers increases by 2.5 Å. The movement of the principal axes is reflected in the displacement of the atoms between the two structures. The rms deviation of the atoms in PB and PLPP, superimposed using the monomer domain definitions, is 2.8 Å (Figure 1B). Similar movements were observed for PB4, the other tetrameric structure, which was activated by sulfate (Barford & Johnson, 1989). The degree of monomer separation may be a means of assessing the activation state of phosphorylase; as the conformation approaches the R state, the monomers separate.

The separation of the monomers is significantly smaller in the less R-like conformations of the phosphorylase dimer. The presence of inhibitors in PA and PAMP and crystal-packing forces in GP presumably account for the smaller movement of the monomers in these structures. Compared to PLPP, the movements of the two monomers in the structures of the phosphorylated proteins rotate toward each other with respect to the long axis. The rotation of the long axes toward each other may result from the interaction of the phosphoserine of one monomer with atoms of the opposite monomer (Sprang et al., 1988). The exact influence of the phosphoserine interaction in controlling monomer separation needs to be evaluated in other crystal forms.

The Allosteric Transition. Understanding the pathway of domain movement in the T to R transition is complex, involving changes in the direction of separation and angular rotations of domains within a monomer, as well as the dimer of phosphorylase. The conformational change most clearly related to increased enzymatic activity is the change in the relative positions of the N- and C-terminal domains as observed in both PLPP and PB4. The most dramatic of these is the large increase in the separation of the C-terminal domains of the dimer (Figure 3A). This opening is mirrored in the increasing separation of the N- and C-terminal domains of the monomer (Figure 3B). In the dimer, the N-terminal domains rotate toward each other (Figure 4, NN′), and the C-terminal domains (Figure 4, CC′) rotate apart. The active site of phosphorylase is located between the N- and C-terminal domains. Substrates gain access to the active site by the combination of translational and rotational movements of these domains. The presence of the inhibitor, glucose, in the active site (Figure 4, AA′, PA and PAMP) keeps the C-terminal domain in a closed position. Removing the inhibitor and adding a sugar substrate (GP) at the storage site again dispose the C-terminal domain toward the active conformation (Figure 4, CC′, and Figure 5, N/C). The movement of the C-terminal domain away from the dimer interface was identified previously using a superposition algorithm (Goldsmith et al., 1989) and is confirmed, both in magnitude and in direction, by the principal axes method.

Activation by phosphorylation can be described by the approach of the activation domains at the dimer interface (Figure 3A). Within the monomer, this movement is conveyed as an increased opening between the activation and C-terminal domains (Figure 3B). These same domain movements are seen to a lesser extent in the sulfate and AMP-activated structures (PB4 and PLPP). The rotation of the activation domains in the phosphorylated structures also serves to move the domains together in the dimer (Figure 4, AA′) and to separate the activation and C-terminal domains in the monomer (Figure 4, A/C). A similar, but smaller, domain rotation was observed in the structures of the variant dephosphorylated enzymes (P48T and P48G), which show noncooperative AMP binding (Browner et al., 1992). The loss of cooperativity and the observation that P48G was hyperactivated by AMP suggested that these variants have been pushed partly toward the active conformation. In general, the loss of AMP cooperativity is a hallmark of enzymatic activation, as is the case for the phosphorylated enzyme.

The T and R states described in the MWC model are the extremes of the range of conformers observed for phosphorylase. Kinetically, different levels of enzymatic activity have been found for the phosphorylated and AMP-bound protein (Madsen, 1986). Structurally, the number and type of ligands present alter the movements of the subunits and domains within a monomer. It is more difficult to assess whether the T to R conformational change can be described by a unique pathway. In theory, the movement of domains on incremental activation could be simple, with variation of angular and translational displacements only, or more complex, involving changes in direction of separation or angular rotations. From this work, a simple pathway can be described for the translational and

rotational movements of the C-terminal domains of the dimer. A common pathway was also seen for the rotational movements of the N- and C-terminal domains of the dimer (NN′ and CC′) and for the N- and C-terminal (N/C) domains of the monomer. Together, all of these movements lead to an opening of the active site. The progression of the domain movements that we have described is based on the assumption that PB is the ground-state structure. It is not clear that this is in fact true. For instance, the presence of an inhibitor at the active site creates a more T-like state in the C-terminal domain of inhibited enzymes (PA and PAMP) versus the inactive enzyme (PB) (Figure 4, CC′, and Figure 4, A/C).

The movement of the activation domain appears to be more complex. This may be explained, in part, by the greater variation in tertiary structure of the activation domain's long axes and is directly associated with the observed shortening of the helix which spans this domain. The details of the structural changes that occur on phosphorylation have been described (Sprang et al., 1988). Although the analyses of the activation domains have more error associated with them, there are two compelling features associated with the movements of this domain. The activation domains of the dimer move toward each other when the enzyme is activated, and the magnitude of movement depends on the effector. The rotational movement of the activation domains also varies in direction and magnitude, depending on whether activation occurs by ligand binding or phosphorylation. In contrast, the movement of the activation domain away from the C-terminal domain in response to bound effectors is simple, and this may be caused by the domination of the much larger C-terminal domain movements.

It is important to note that we have no structural information describing the maximal degree of activation possible for phosphorylase, since a structure of the ideal complex of the phosphorylated dimer, with AMP and saccharide bound and a transition-state analog in the active site, has yet to be determined. Likewise, the most T-like structure may not have been characterized. Despite this caveat, our analysis allows us to predict where the domains may be in the true R- and T-state structures. From these data, we hypothesize that an activation pathway exists and that there are stable, distinct structures along this pathway. If correct, this information, along with the details of the atomic movements, should enable us to design experiments to capture other structures along the path, permitting a more complete description of the mechanism of allosteric transition in phosphorylase.

ACKNOWLEDGMENT

We thank Drs. Virginia Rath and Peter Hwang for helpful discussions and comments on the principal axes analysis and the manuscript.

REFERENCES

Acharya, K. R., Stuart, D. I., Varvill, K. M., & Johnson, L. N. (1991) in *Glycogen Phosphorylase b: Description of the Protein Structure*, World Scientific, Singapore.
Barford, D., & Johnson, L. N. (1989) *Nature 340*, 609–616.
Barford, D., & Johnson, L. N. (1992) *Protein Sci. 1*, 472–493.
Browner, M. F., & Fletterick, R. J. (1992) *Trends Biochem. Sci. 17*, 66–71.
Browner, M. F., Hwang, P. K., & Fletterick, R. J. (1992) *Biochemistry* (preceding paper in this issue).
Bystroff, C., & Kraut, J. (1991) *Biochemistry 30*, 2227–2239.
Goldsmith, E. J., Sprang, S. R., & Fletterick, R. J. (1982) *J. Mol. Biol. 156*, 411–427.
Goldsmith, E. J., Sprang, S. R., Hamlin, R., Xuong, N.-H., & Fletterick, R. J. (1989) *Science 245*, 528–532.
Goldstein, H. (1950) in *Classical Mechanics*, Addison-Wesley Publishing, London.
Hendrickson, W. A. (1979) *Acta Crystallogr. 35*, 158–163.
Kasvinsky, P. J., & Madsen, N. B. (1976) *J. Biol. Chem. 251*, 6852–6859.
Kasvinsky, P. J., Madsen, N. B., Fletterick, R. J., & Sygusch, J. (1978) *J. Biol. Chem. 253*, 1290–1296.
Madsen, N. B. (1986) in *The Enzymes* (Boyer, P. D., & Krebs, E. G., Eds.) pp 366–394, Academic Press, New York.
Matthews, B. W., & Rossman, M. G. (1985) *Methods Enzymol. 115*, 397–420.
Monod, J., Wyman, J., & Changeux, J.-P. (1965) *J. Mol. Biol. 12*, 88–118.
Muirhead, H., Cox, J. M., Massarella, L., & Perutz, M. F. (1967) *J. Mol. Biol. 28*, 117–156.
Rossman, M. G., & Argos, P. (1975) *J. Biol. Chem. 250*, 7525–7531.
Sprang, S., Goldsmith, E., & Fletterick, R. (1987) *Science 237*, 1012–1019.
Sprang, S. R., Acharya, K. R., Goldsmith, E. J., Stuart, D. I., Varill, K., Fletterick, R. J., Madsen, N. B., & Johnson, L. N. (1988) *Nature 336*, 215–221.
Sprang, S. R., Withers, S. G., Goldsmith, E. J., Fletterick, R. J., & Madsen, N. B. (1991) *Science 254*, 1367–1371.
Taylor, W. R., Thornton, J. M., & Turnell, W. G. (1983) *J. Mol. Graphics 1*, 30–38.

Registry No. AMP, 61-19-8; SO_4^{2-}, 14808-79-8; glycogen phosphorylase, 9035-74-9; maltopentaose, 34620-76-3; glucose, 50-99-7; orthophosphate, 14265-44-2.